Article

Cite This: *Biomacromolecules* 2018, 19, 4122−4132

pubs.acs.org/Biomac

Nucleus-Targeted, Echogenic Polymersomes for Delivering a Cancer Stemness Inhibitor to Pancreatic Cancer Cells

Fataneh Karandish,[†] Babak Mamnoon,[†] Li Feng,[†] Manas K. Haldar,[†] Lang Xia,[‡] Kara N. Gange,[§] Seungyong You,[∥] Yongki Choi,[∥] Kausik Sarkar,[‡] and Sanku Mallik*[,†]

[†]Department of Pharmaceutical Sciences, [§]Department of Health, Exercise, and Nutrition Sciences, and [∥]Department of Physics, North Dakota State University, Fargo, North Dakota 58108, United States

[‡]Department of Mechanical and Aerospace Engineering, The George Washington University, Washington, D.C. 20052, United States

Supporting Information

ABSTRACT: Chemotherapeutic agents for treating cancers show considerable side effects, toxicity, and drug resistance. To mitigate the problems, we designed nucleus-targeted, echogenic, stimuli-responsive polymeric vesicles (polymersomes) to transport and subsequently release the encapsulated anticancer drugs within the nuclei of pancreatic cancer cells. We synthesized an alkyne-dexamethasone derivative and conjugated it to N_3−polyethylene glycol (PEG)−polylactic acid (PLA) copolymer employing the Cu^{2+} catalyzed "Click" reaction. We prepared polymersomes from the dexamethasone−PEG−PLA conjugate along with a synthesized stimuli-responsive polymer PEG−S−S−PLA. The dexamethasone group dilates the nuclear pore complexes and transports the vesicles to the nuclei. We designed the polymersomes to release the encapsulated drugs in the presence of a high concentration of reducing agents in the nuclei of pancreatic cancer cells. We observed that the nucleus-targeted, stimuli-responsive polymersomes released 70% of encapsulated contents in the nucleus-mimicking environment in 80 min. We encapsulated the cancer stemness inhibitor BBI608 in the vesicles and observed that the BBI608 encapsulated polymersomes reduced the viability of the BxPC3 cells to 43% in three-dimensional spheroid cultures. The polymersomes were prepared following a special protocol so that they scatter ultrasound, allowing imaging by a medical ultrasound scanner. Therefore, these echogenic, targeted, stimuli-responsive, and drug-encapsulated polymersomes have the potential for trackable, targeted carrier of chemotherapeutic drugs to cancer cell nuclei.

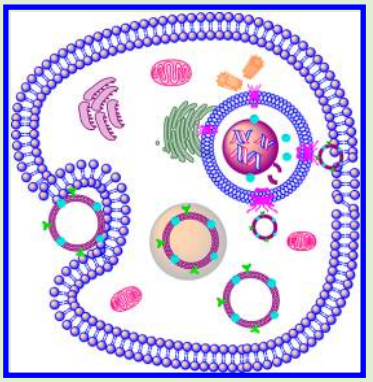

INTRODUCTION

Pancreatic ductal adenocarcinoma (PDAC) is the fourth leading cause of death in the United States with the approximate five-year survival rate of less than 10%.[1] Pancreatic cancer treatment is complicated because of invasiveness, rapid metastasis, and the complex nature of the disease. Alteration of different genes, aberrant biochemical pathways, epithelial to mesenchymal transition (EMT), hypoxic tumor microenvironment, and the subpopulation of cancer stem cells lead to recurrence and drug resistance.[2] Considering that pancreatic cancer shows early invasion and metastasis, there is an urgent need for developing new treatment of this devastating disease. In the solid tumor tissue, EMT leads to a subpopulation of cancer stem cells, which can initiate a tumor, self-renew, and increase resistance to chemotherapeutic drugs.[3] The small molecule BBI608 (napabucasin) inhibits signal transducer and activator of transcription 3 (STAT3), reduces the expression of cancer stemness markers, inhibits cell proliferation, and blocks spherogensis and apoptosis in both cancer stem cells and nonstem cells.[2−4] BBI608 is currently in the Phase III clinical trials as an adjuvant therapy for a variety of solid tumors, including pancreatic cancer (www.clinicaltrials.gov). STAT3 controls many oncogenic pathways and is activated in different type of cancers such as breast, ovarian, colorectal, and so on.[4]

Targeted, stimuli-responsive carriers enhance therapeutic efficacy and reduce toxicity by selectively delivering the cytotoxic chemotherapeutic drugs to cancerous tissues.[5−7] Polymersomes are vesicles prepared from synthetic, amphiphilic block copolymers. Because of higher molecular weights, polymersomes have enhanced stability and mechanical robustness compared to liposomes, micelles, and polymer micelles.[8] The bilayer of the polymersomes encapsulate hydrophobic drugs, and the aqueous core incorporates the hydrophilic molecules, enabling simultaneous delivery of both drugs.[9] Conjugation of antibodies, small molecules or peptides enables active targeting of the vesicles to the cancer cells.[10,11] However, due to increased stability, the polymer bilayer usually requires a stimulus to rapidly release the encapsulated anticancer drugs.[12] Polymersomes responsive to pH,[13] heat,[14] hypoxia,[15] and light[16] has been used to deliver chemotherapeutic drugs to the cancer cells. Multifunctional polymersomes with drug delivery

Received: July 24, 2018
Revised: August 27, 2018
Published: August 31, 2018

DOI: 10.1021/acs.biomac.8b01133
Biomacromolecules 2018, 19, 4122−4132

Scheme 1. [2 + 3]-Cycloaddition Reaction of N_3−PEG_{1900}−PLA_{8000} Polymer and Alkyne-Dexamethasone

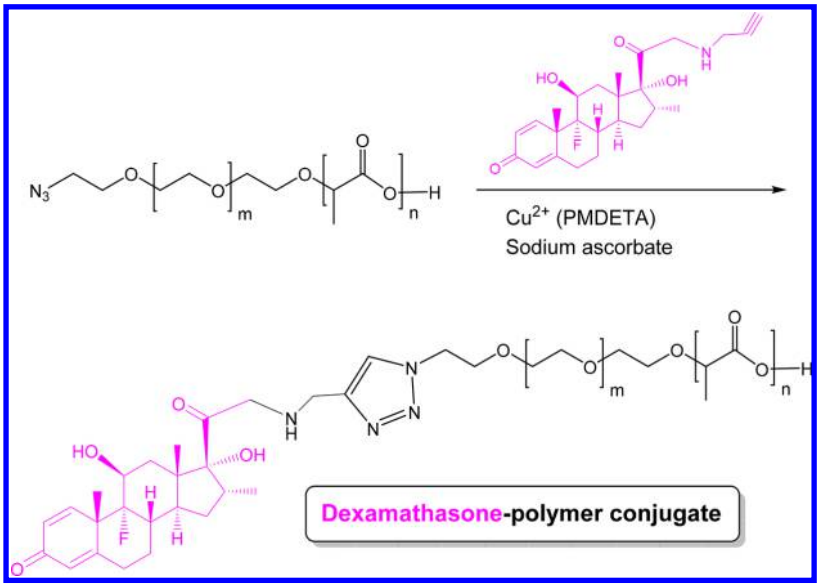

and simultaneous imaging capability are also reported.[17,18] The polymeric nanoparticles accumulate in the tumor tissues by the enhanced permeation and retention effect;[19] however, for efficient cellular internalization, specific ligands are necessary on the vesicle surface.

Nuclear pore complex is a large multiprotein assembly, which spans the nuclear envelope. Approximately 2000 nuclear pore complexes exist in the nuclear envelope. Dexamethasone is a synthetic steroid that dilates the nuclear pore complex from 38 to 300 nm.[20,21] Glutathione (GSH), the abundant cellular reducing agent, is a tripeptide consisting of glutamic acid, cysteine, and glycine. GSH is involved in several important processed in the cell nuclei, such as transcription, DNA replication, nuclear protein import and export, and chromatin stability.[22,23] High levels of GSH are related to increased cell proliferation.[2324]

Herein, we report nucleus-targeted, echogenic, redox-sensitive polymersomes to deliver the cancer stemness inhibitor BBI608 to pancreatic cancer cells. We used dexamethasone as a targeting group to dilate the nuclear pore complexes[19] and deliver the polymersomes inside the nucleus. In the synthesized copolymer, we used polyethylene glycol (PEG) as the hydrophilic block and polylactic acid (PLA) as the hydrophobic block. Incorporation polyethylene glycol polymer (PEGylation) in the polymersomes composition reduces the interactions of nanoparticle with circulating proteins.[25] Polylactic acid (PLA) is the hydrophobic part of the polymer and has a degradation time of more than 1 week in aqueous solutions at 37 °C.[26,27] The two polymer blocks were linked by the reduction sensitive disulfide linker. Several literature reports demonstrate the effectiveness of the disulfide bonds to deliver the encapsulated payloads under increased cellular reducing agent concentration[28−31] We observed that the vesicles, presenting dexamethasone on the surface, internalize in the nuclei of pancreatic cancer cells. The high reducing agent concentration in the nuclei[32,33] cleaves the disulfide bonds of the polymers, compromises the polymersome structure, and rapidly releases the encapsulated drug. We observed that nucleus-targeted polymersomes encapsulating BBI608 significantly ($p < 0.05$) decreased the viability of the BxPC3 cells compared to control and the nontargeted vesicles. The polymersomes were shown to be responsive to ultrasound offering possibility of concurrent ultrasound imaging of the cancerous tumors. We have used a preparation protocol incorporating lyophilization in the presence of mannitol that has proved previously effective in rendering liposomes[34−39] and polymersomes[40] echogenic.

MATERIALS AND METHODS

All chemicals and solvents were purchased either from VWR International or TCI America and used as received.

Synthesis of Alkyne-Dexamethasone. Dexamethasone (100 mg, 0.26 mmol) was dissolved in anhydrous pyridine (2 mL) in a round-bottom flask and stirred on ice (0 °C) with methane sulfonyl chloride (250 μL, 3.2 mmol) under nitrogen for 4 h. Then, an additional amount of methane sulfonyl chloride (18 μL, 0.23 mmol) was added, and the reaction continued for an additional hour. After 5 h of stirring under nitrogen, 40 mL of ice water was added to precipitate the product. The precipitate was filtered and washed with 40 mL of additional ice water. The crude product was purified by recrystallization from tetrahydrofuran (THF) twice to afford the pure product. The product (0.026 g, 0.06 mmol) and propargylamine (0.10 mL, 1.561 mmol) were stirred in 800 μL of dimethylformamide (DMF) at 65 °C under nitrogen gas for 2 h. After cooling to room temperature, the reaction mixture was added dropwise to cold water and centrifuged at 425 g for 10 min. The clear supernatant was decanted, and the precipitate was washed again with water and dried under vacuum. The pure product (16 mg, 62%) was characterized by ^{1}H NMR spectroscopy (Supporting Information). ^{1}H NMR (400 MHz, chloroform-d) δ ppm: 7.41 (d, 1H), 6.40 (d, 1H), 6.20 (d, 1H), 4.37 (d, 2H), 4.32 (t, 1H), 3.41 (s, 1H), 2.43 (t, 2H), 2.38 (t, 2H), 1.70 (d, 2H), 1.56 (s, 3H), 1.06 (s, 3H), 0.95 (s, 3H). HRMS Calcd for C_{25} $H_{32}FNO_4$, 429.2315; Observed, 429.2306.

Synthesis of Dexamethasone−PEG1900−PLA8000 Polymer Conjugate. We synthesized the N_3−PEG_{1900}−PLA_{8000} polymer employing a protocol developed in our laboratory (Supporting Information). The alkyne-dexamethasone was reacted with the N_3−PEG_{1900}−PLA_{8000} polymer using the [2 + 3]-cycloaddition reaction (Scheme 1).[41] Briefly, we prepared the copper(II) complex by mixing the $CuSO_4$ (71.3 mg in 3 mL of water, 0.53 mmol) and pentamethyl diethylenetriamine (440 μL in 3 mL water, 2 mmol). The N_3−PEG_{1900}−PLA_{8000} polymer (20 mg) and alkyne-dexamethasone (2 mg) were dissolved in 6 mL of tetrahydrofuran (THF), 400 μL of the 53 mM copper complex and 400 μL of 53 mM aqueous sodium ascorbate solution were added, and the reaction mixture was stirred at

DOI: 10.1021/acs.biomac.8b01133
Biomacromolecules 2018, 19, 4122−4132

room temperature for 24 h. The reaction mixture was added dropwise to cold ether and centrifuged at 425*g* for 2 min. The clear supernatant was decanted, and the precipitate was washed with water three times by vortex and centrifuge, and then dried under vacuum. ^{1}H NMR (400 MHz, chloroform-*d*) δ ppm: 6.34 (d, 1H), 6.15 (d, 1H), 5.18 (q, 1 H), 4.37 (d, 2H), 3.66 (t, 4 H), 2.52 (t, 2H), 2.30 (t, 2H), 1.60 (d, 3 H). From the ^{1}H NMR spectrum, we calculated the conversion yield for the dexamethasone coupling reaction to be 39% (Supporting Information).

Preparation of Nucleus Targeted Polymersomes Encapsulating BBI608. Polymersomes were prepared by the solvent exchange method[42] with PEG_{1900}−S−S−PLA_{6000},[43] dexamethasone−PEG_{1900}−PLA_{8000} polymer, and 1,2-dipalmitoyl-*sn*-glycero-3-phosphoethanolamine-*N*-lissamine rhodamine B sulfonyl ammonium salt (fluorescent dye, LR, Avanti Polar Lipids) with a molar ratio of 35:60:5, respectively (Figure 2). The polymers were dissolved in THF (9 mg/mL), BBI608 in THF (3 mg/mL), and LR in chloroform (0.01 mg/mL). First, a rotary evaporator was used to evaporate the chloroform from LR lipid to form a thin layer film. The THF solutions of the polymers and BBI608 were added to the thin film. The resultant fluorescent THF solution was added dropwise to an aqueous HEPES buffer (10 mM, pH 7.4) and stirred for 45 min. To remove the THF, a gentle stream of air was passed through the mixture for 45 min. The polymersomes formed were bath sonicated for 60 min (Symphony 117 V, 60 Hz, Power level 9). The polymersomes (1 mg/mL) were passed through a Sephadex G-100 size exclusion column to remove the unencapsulated drug. Drug loading efficacies (DLE) of the polymersomes were determined using UV−vis spectroscopy. After passing through the size-exclusion column, the absorption of the polymersomes was recorded at 235 nm to calculate the loading efficiency.

Preparation of Control Polymersomes. The control polymersomes were prepared following the same method as the nucleus-targeted vesicles. PEG_{1900}−S−S−PLA_{6000}, N_3−PEG_{1900}−PLA_{8000}, and lissamine rhodamine (LR) were used in the molar ratio of 35:60:5, respectively. The PEG_{1900}−S−S−PLA_{6000} and N_3−PEG_{1900}−PLA_{8000} polymers were dissolved in THF. The polymer solution was added slowly to the thin film of the LR dye, and then the mixture was added dropwise to a stirred 10 mM HEPES buffer (pH 7.4). The polymersome solutions were stirred for 45 min at room temperature, and then air was passed for 45 min through the mixture. The polymersomes were sonicated for 60 min (Symphony 117 V, 60 Hz). Subsequently, the polymersomes were passed through a Sephadex G100 (GE Healthcare) size exclusion column to collect lissamine rhodamine dye incorporated polymersomes. These polymersomes were used as a control for the cell viability assays.

Polymersomes Size Analysis. The nucleus-targeted polymersomes encapsulating BBI608 and control polymersomes were characterized by dynamic light scattering at 90° using a Zeta Sizer Nano ZS 90 (Malvern Instrument). Polymersomes were equilibrated for 120 s, and five measurements were recorded with 10 repeats each.

Transmission Electron Microscopy (TEM). Samples were prepared on 300 mesh copper grids with a Formvar-carbon support film. Grids were pretreated with 1% poly-L-lysine and air-dried; 5 μL of the polymersome suspension was added and allowed to stand 1 min, then wicked off with a filter paper. Negative staining was performed using 0.1% phosphotungstic acid for 2 min, then wicking off and air-dried before observation and imaging in a JEOL JEM-2100 LaB_6 transmission electron microscope.

Atomic Force Microscopic (AFM) Imaging. The size and morphology of polymersomes were characterized using atomic force microscopy. Polymersomes (1 mg/mL) were diluted (20×) in HEPES buffer (pH 7.4, 10 mM). Polymersomes were dropped on silica substrates, incubated for a minute, and extra liquid dried by an air blowgun. The AFM measurements were performed in noncontact mode (resonance frequency of 145 kHz and a scanning rate of 1.3 Hz) using an NT-MDT INTEGRA instrument (NT-MDT America). The scanning areas were 5 × 5 μm^2 at the resolution of 512 points per line, respectively. The images were flattened to eliminate the background low-frequency noise and tilt from the surface using all unmasked portions of scan lines to calculate individual least-squares fit polynomials for each line.

Redox-Triggered Release Studies. Polymersomes encapsulating 20 μM calcein dye were prepared to perform the release study. The experiments were conducted by the quenching method[44] using cobalt chloride as the quencher and glutathione as the reducing agent. The cobalt(II) chloride (10 mM) was used to quench the fluorescence from the unencapsulated calcein outside the vesicles. We used 20 μL of calcein-encapsulated polymersomes (total polymer concentration: 1 mg/mL) in 10 mM HEPES buffer (180 μL, pH = 7.4) in a 96-well plate. The release from the polymersomes were monitored in the presence of 10 mM glutathione for 40 min; subsequently, the concentration was increased to 50 mM, and the release was monitored for an additional 40 min (excitation: 495 nm, emission: 515 nm) employing a fluorescence microplate reader (Spectramax M5, Molecular Devices). The amount of calcein release form polymersomes were calculated employing this equation:

$$\%\ \text{release} = [(\text{emission intensity after 80 min} - \text{initial intensity before treatment}) / \text{initial intensity before treatment}] \times 100$$

Preparation and Characterization of Echogenic Polymersomes. Polymersomes were prepared by dissolving the PEG_{1900}−S−S−PLA_{6000} and N_3−PEG_{1900}−PLA_{8000} polymers with the molar ratio of 40:60 (total 5 mg in 1 mL of THF), respectively. Then, the polymer mixture was dropwise added to 0.32 M mannitol (weak cryoprotectant) prepared in HEPES buffer (10 mM, pH 7.4). Subsequently, THF was evaporated for 45 min by passing air through the solution. Then, polymersomes were sonicated for 60 min (Symphony 117 V, 60 Hz). To make the polymersomes echogenic, they were subjected to three freeze (−80 °C, 24 h) and thaw (60 °C) cycles. Finally, the polymersomes were lyophilized (Labconco freeze-dryer) and reconstituted in HEPES buffer (10 mM, pH 7.4) for further experiments.

Ultrasound Experimental Setup to Measure Scattering in Echogenic Polymersomes. Two spherically focused transducers (each having a central frequency of 2.25 MHz/5 MHz/10 MHz, Figure 3) with the same specifications (V310-SU, Olympus NDT) were employed for scattering measurements. The transmitting and receiving transducers were placed perpendicularly by two separate linear stages (433 series, 360−90, Newport) and immersed in a bigger water tank filled with DI water. A 20 mL syringe served as a sample chamber, in which polymersome suspension was injected. A function generator (Model AFG 3251; Tektronix) was utilized to generate a 32-cycle sinusoidal pulse of 5 MHz frequency at a PRF of 100 Hz. These signals were then amplified using a 55 dB power amplifier (Model A-300, ENI) and sent to the transmitting transducer. The input signals were scattered by the polymersomes inside the focal volume of the transducer. The scattered signals were received by the receiving transducer connected to a pulser/receiver (DPR300, 475v, JSR) in the through mode with a 27 dB gain. The output signals were then transmitted to an oscilloscope (TDS2012, Tektronix) for real-time visualization. The output voltage−time RF signals were obtained by the oscilloscope by averaging over every 64 sequences. The data from the oscilloscope were finally transmitted and saved onto a desktop computer using the software Signal Express Tektronix Edition (version 2.5.1, Labview NI). In time-dependent scattering experiments, all the setups and procedures were the same except that the data were recorded over a 20 min period (corresponding to about 344 acquisitions). As for the degassed experiment, all the setups and procedures were still the same, only difference being that the PBS solution had been degassed using a vacuum pump.

Echogenic Polymersomes' Experimental Procedure and Data Reduction. In a scattering experiment, the suspension was made by reconstituting the dry powder in phosphate buffered saline (PBS) solution to obtain a concentration of 10 μg polymer/mL. We injected 20 mL of the resulting suspension into the sample chamber. The measurement was repeated five times to guarantee the reliability of the experimental data. The measurement of the control signal, that

DOI: 10.1021/acs.biomac.8b01133
Biomacromolecules 2018, 19, 4122−4132

is, without polymersomes and the responses due to the polymersomes were acquired by the procedures above. The Fourier transform of the signal was performed using a Matlab program to get the average scattered power spectra in the frequency domain (50 voltage time acquisitions were used for averaging). The scattered response was converted into a dB scale by taking a unit reference. Fundamental, second- and subharmonic scattered responses were extracted from the power spectrum. The final data is reported as an enhancement over the control. We also checked the scattered response in the presence of 50 mM of glutathione.

Ultrasound Imaging. Dried polymersomes were reconstituted in 10 mM HEPES buffer, pH 7.4 with the concentration of 10 μg/mL. In a 96-well plate, 0.2 mL of polymersomes were dispensed into each well; then the plate was covered with parafilm. Subsequently, an ultrasound gel (Aquasonic 100, Parker Laboratories) was applied, and a 15 MHz linear ultrasound transducer was used for the imaging experiments employing a Terason t3200 instrument (MediCorp LLC).

Cell Culture. The pancreatic cancer cell line BxPC3 was purchased from the American Tissue Culture Consortium (ATCC). The cells were maintained in RPMI 1640 medium (without phenol red) supplemented with 1% v/v antibiotics (penicillin and streptomycin) and 10% v/v fetal bovine serum. The cell culture flasks were maintained in an incubator at 37 °C in a 5% CO_2 atmosphere.

Nuclear Uptake Studies. The BxPC3 cells (3×10^3) were seeded in a 12-well tissue culture plate for 24 h before the experiment. Once the culture is 80−90% confluent, the nucleus-targeted (20 μL) and nontargeted (20 μL) polymersomes were incubated with the cells for 3 h. Subsequently, the cell culture media and polymersomes were removed, and the cells were washed twice with Hanks' balanced salt solution (HBSS) to remove the noninternalized vesicles. The cell nuclei were stained with HOESCHT 33342 dye (Enzo Life Sciences, 1:1000 dilution) and imaged using the 20× objective of a Leica fluorescence microscope.

Cell Viability in Monolayer Cultures. To evaluate the efficacy of the nucleus-targeted polymersomes on the human pancreatic cancer cells (BxPC3), the Alamar Blue assay was performed. The BxPC3 cells were seeded at a density of 10^3/well in a 96-well tissue culture plate and were allowed to grow until 80−95% confluent. The plate was divided into four groups: control, free drug (BBI608), nontargeted polymersomes, and nucleus-targeted polymersomes encapsulating BBI608. The control group did not receive any treatment. Cells treated with BBI608 received 1, 4, and 8 μM of free and an equivalent amount of encapsulated drug in nucleus-targeted polymersomes. The cells were treated for 48 h at 37 °C, in a 5% CO_2 atmosphere. Subsequently, the cells were washed with sterile HBSS and replaced with 200 μL of fresh media. Then 20 μL of Alamar Blue was added to all the wells and fluorescence were measured after 4 h. The data presented are normalized to the control.

Cell Viability in Three-Dimensional (3D) Spheroid Cultures. The 24-well 3D Petri dishes (Microtissues) were used to prepare BxPC3 spheroids. Briefly, 2% w/v agarose solution was prepared and autoclaved. The BxPC3 cell suspension (10^4 cells in 60 μL of media) was then added to each 3D scaffold. The spheroids were allowed to grow for 7 days. Then scaffolds were divided into four groups: control, nontargeted polymersomes, nucleus-targeted polymersomes encapsulating BBI608, and free drug. Spheroids were treated for 48 h with the same concentration of drug as used for the monolayer studies. Subsequently, the spheroids were washed with sterile HBSS and then incubated with 100 μL of TryPLE (recombinant trypsin, Life Technologies) for 10 min. The spheroids were removed and subjected to the Alamar Blue assay. The data presented are normalized to the control.

RESULTS AND DISCUSSION

Polymer Synthesis and Polymersome Preparation. To prepare nucleus targeted polymersomes, we synthesized an alkyne-dexamethasone conjugate (Figure 1) and linked it to the N_3-−PEG_{1900}−PLA_{8000} polymer (Figure 2 and Supporting Information). The redox-sensitive polymer PEG_{1900}−S−S−PLA_{6000} (Figure 2) was synthesized as previously reported by our group.[15,43,45] The dexamethasone−PEG_{1900}−PLA_{8000} polymer conjugate was synthesized using the Click chemistry

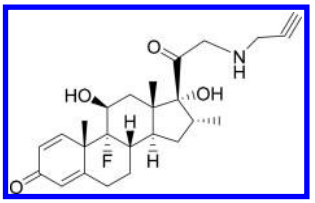

Figure 1. Structure of the synthesized alkyne conjugated dexamethasone.

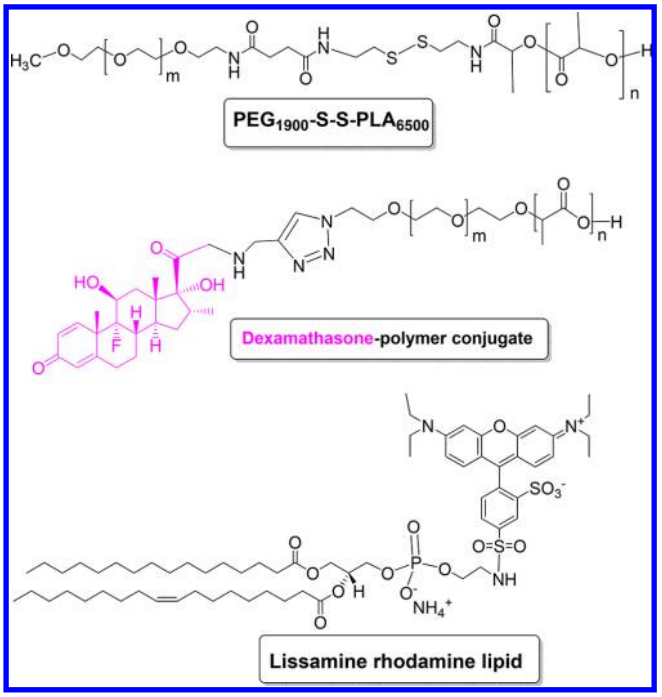

Figure 2. Structure of synthesized polymers PEG_{1900}−S−S−PLA_{6000}, dexamethasone−PEG_{1900}−PLA_{8000} polymer conjugate, and the commercially available fluorescent lipid 1,2-dipalmitoyl-*sn*-glycero-3-phosphoethanolamine-*N*-lissamine rhodamine B sulfonyl ammonium salt.

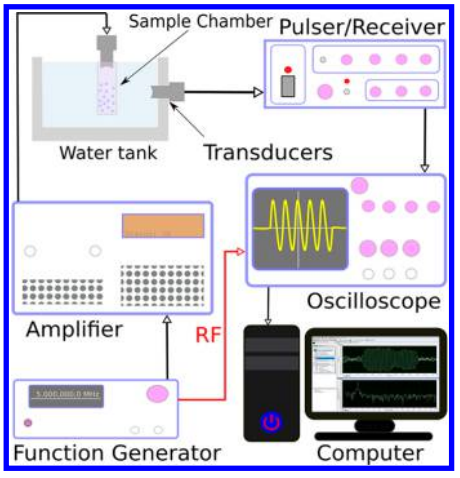

Figure 3. Experimental setups for the ultrasound scattering measurements from the echogenic polymersomes.

DOI: 10.1021/acs.biomac.8b01133
Biomacromolecules 2018, 19, 4122−4132

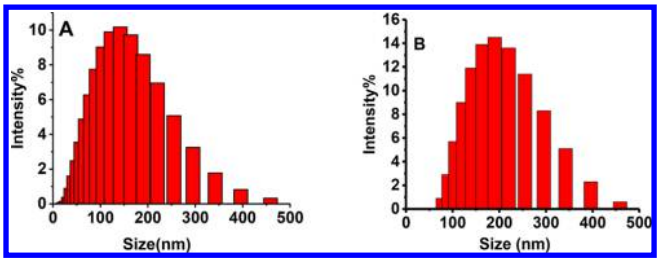

Figure 4. Hydrodynamic diameters of the (A) nontargeted and (B) nucleus-targeted polymersomes encapsulating the stemness inhibitor BBI608, as determined by dynamic light scattering.

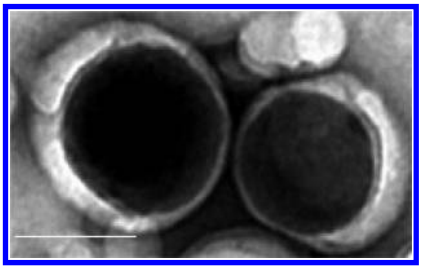

Figure 5. Transmission electron microscopy images (scale bar: 50 nm) of the nontargeted polymersomes.

[2 + 3 cycloaddition]. We anticipated that the slightly higher molecular weight of the polymer conjugate would protrude the dexamethasone group from the surface of the vesicles and facilitate the interactions with its receptor. The polymersomes were prepared by the solvent exchange method[42] and characterized by dynamic light scattering (Figure 4), transmission electron microscopy (Figure 5), and atomic force microscopy (Figure 6). We encapsulated the stemness gene transcription inhibitor BBI608 (napabucasin)[3] in the polymersomes with an efficiency of 68 ± 5%. We observed that the nucleus-targeted polymersomes had a hydrodynamic diameter

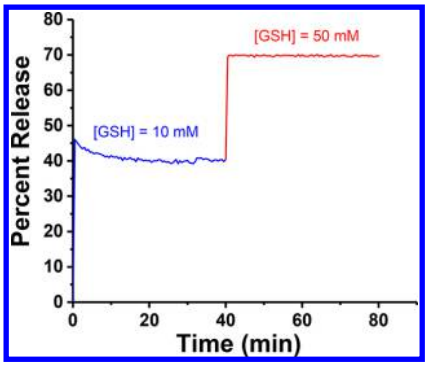

Figure 7. Glutathione-triggered release of the encapsulated calcein from the polymersomes.

of 200 ± 2 nm, with a polydispersity index (PDI) of 0.2 ± 0.02. The average hydrodynamic diameter for the nontargeted polymersomes was 140 ± 3 nm with a PDI of 0.2 ± 0.03. The nucleus-targeted polymersomes were slightly larger than nontargeted polymersomes. We hypothesize that the encapsulation of hydrophobic BBI608 in the polymer bilayer of the vesicles increases the size of vesicles.

The dexamethasone−PEG_{1900}−PLA_{8000} polymer was incorporated into polymersome composition to target the nanoparticles to the cell nucleus. We expected that the dexamethasone on the polymersomes would dilate the nuclear pore complex[21,46] and transport the vesicles into the nucleus. The disulfide bond in the redox-sensitive polymer will subsequently be reduced in the nucleus, releasing the encapsulated BBI608.

Demonstration of Reduction-Triggered Contents Release from the Polymersomes and Structural Characterization. We studied the reduction-triggered release of the dye calcein from the polymersomes as a function of time in the presence of different concentrations of added glutathione

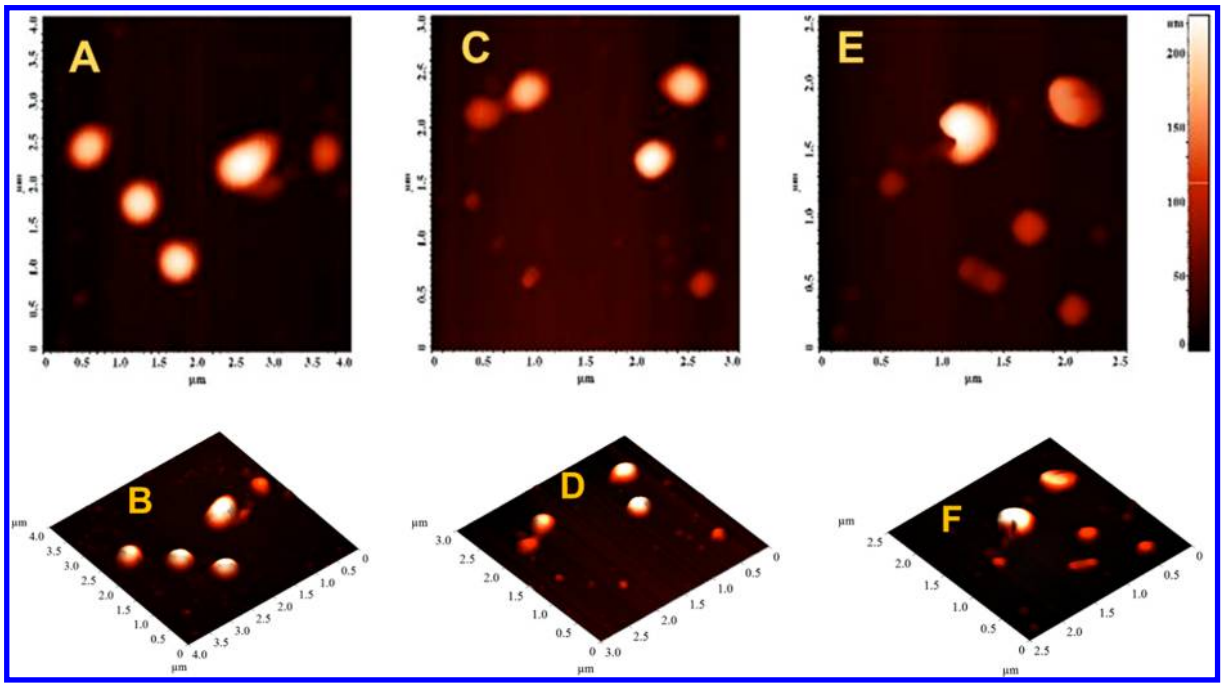

Figure 6. Atomic force microscopy (AFM) images of the nontargeted polymersomes: (A, B) polymersomes, (C, D) polymersomes treated with 10 mM glutathione for 5 min, and (E, F) polymersomes treated with 50 mM GSH for 5 min.

DOI: 10.1021/acs.biomac.8b01133
Biomacromolecules 2018, 19, 4122−4132

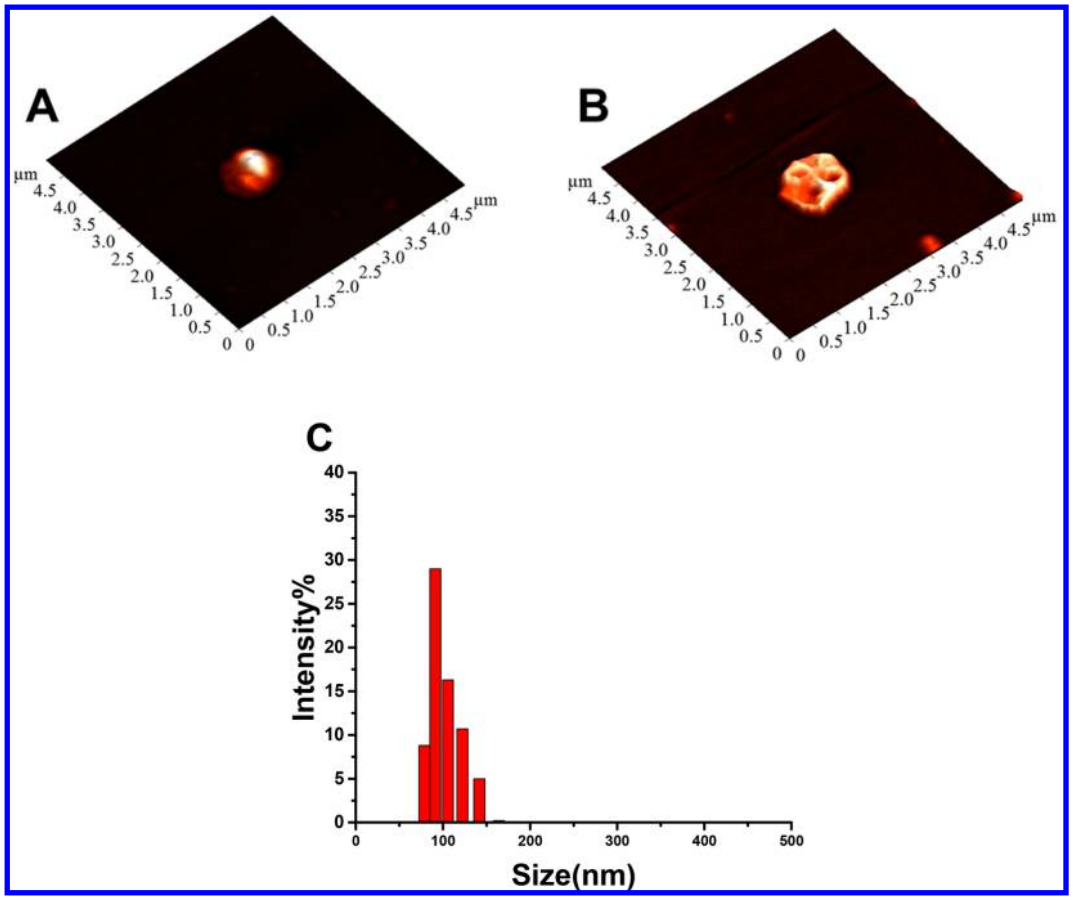

Figure 8. Structural characterization of the polymersomes after release study employing atomic force microscopy. (A) Polymersomes treated with 10 mM GSH. (B) Polymersomes treated with 50 mM GSH. (C) The hydrodynamic diameters of polymersomes after release study, as determined by dynamic light scattering.

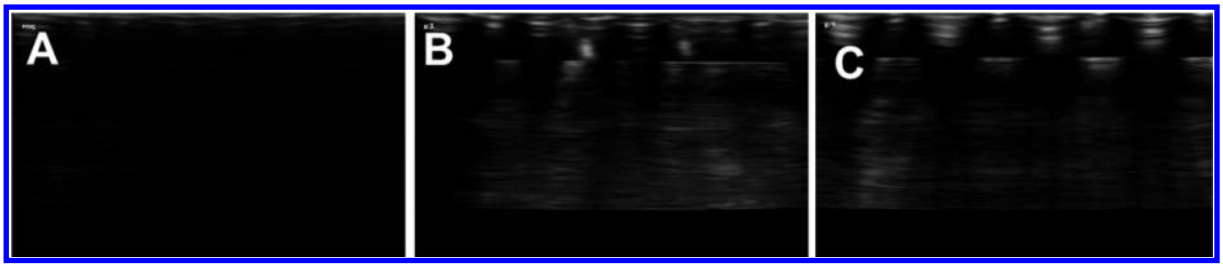

Figure 9. Ultrasound contrast images of the polymersomes at 15 MHz: (A) control, (B) freshly reconstituted echogenic polymersomes, and (C) echogenic polymersomes after 1 week in aqueous solution.

(GSH). GSH is an important intracellular reducing agent, comprising of glutamic acid, cysteine, and glycine.[47] In tumor cells, the concentration of GSH is about 100−1000× higher than the extracellular fluids.[32,48] It is increased level is correlated with progression and proliferation of various cancers, such as breast,[3] colon,[49] lung,[49] pancreas,[47] resistance to chemotherapy.[47] We observed that the polymersomes released 45% the encapsulated dye in the presence of 10 mM (mimicking the cytosol) GSH. However, the released increased to 70% with 50 mM GSH (mimicking the nucleus, Figure 7).[24] We also observed that both of the releases were rapid. Our atomic force microscopic studies indicated that 10 mM GSH slightly changed the morphology of the polymersomes (Figure 8A); however, 50 mM GSH completely disrupted the vesicle structure (Figure 8B). We checked the size of disruption of polymersomes (with dynamic light scattering) and observed that 50 mM GSH decreased the average diameter of the vesicles from 200 nm (Figure 4B) to 100 nm (Figure 8C).

Demonstration of Polymersomes' Echogenicity. Polymersomes' echogenicity was confirmed by a Terason medical ultrasonic imaging system (t3200) using a 15 MHz transducer. We observed that the echogenic polymersomes reflected ultrasound even after a week in the aqueous solution. The ultrasound reflection suggests the presence of air pockets (detailed discussion below) in polymersomes (Figure 9B,C) while control (buffer without any polymersomes) did not show any contrast (Figure 9A).

The scattered power spectra of the polymersomes at three excitation frequencies (2.25, 5, and 10 MHz) are displayed in Figure 10. Power spectra show the responses of the polymersomes as a function of frequencies. Contributions at frequencies other than the excitation frequency indicate

DOI: 10.1021/acs.biomac.8b01133
Biomacromolecules 2018, 19, 4122−4132

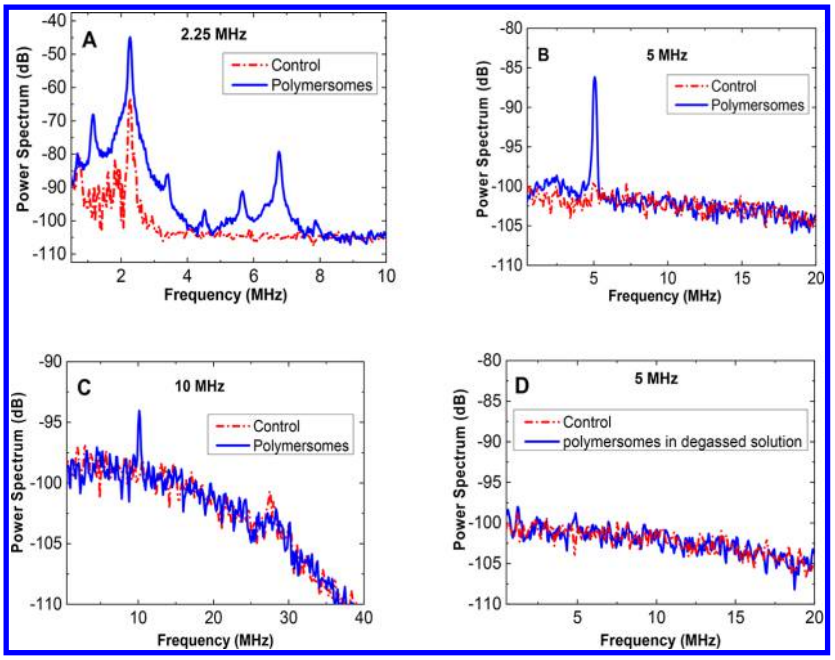

Figure 10. Scattered responses of echogenic polymersomes in PBS at 500 kPa excitation pressure and excitation frequencies of (A) 2.25, (B) 5, and (C) 10 MHz. Control is without polymersomes. (D) Scattered response in degassed solution at 500 kPa and 5 MHz.

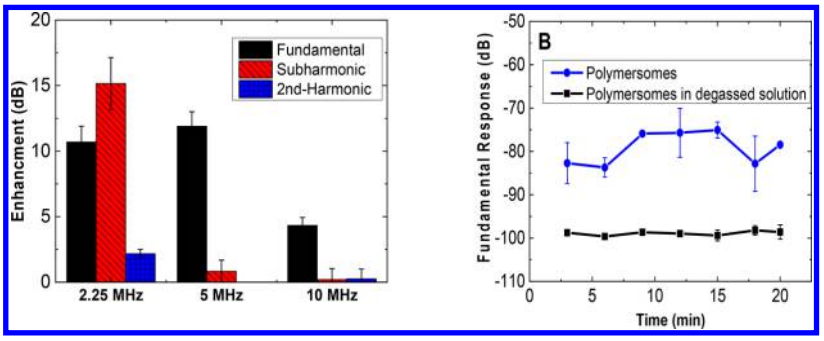

Figure 11. (A) Enhancements in fundamental, sub− and second harmonic scattered responses from the echogenic polymersomes at 500 kPa and 2.25, 5, and 10 MHz. (B) Time-dependent fundamental responses of the echogenic polymersomes in normal (blue trace) and degassed PBS (black trace) at 5 MHz and 500 kPa (N = 5).

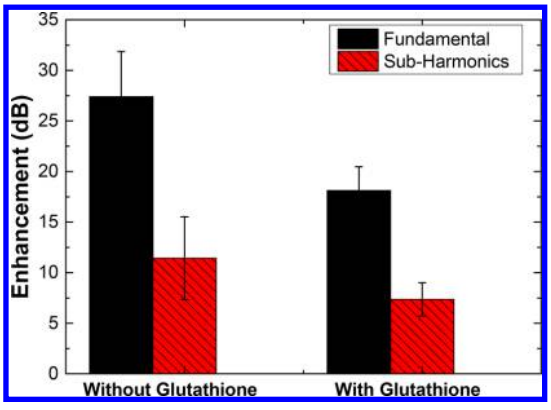

Figure 12. Fundamental (black bars) and subharmonic (red bars) enhancements of echogenic polymersomes at 5 MHz and 500 kPa with and without glutathione.

nonlinear responses of the polymersomes, which in turn offers the possibility of a nonlinear imaging modality with a potentially better signal-to-noise ratio.[50,51] Polymersomes are echogenic in aqueous phosphate buffered saline (PBS, pH = 7.4), but not in the degassed solution (Figure 10D). There is a significant nonlinear response, specifically subharmonic, only at 2.25 MHz (Figure 10A).

Note that although echogenicity of echogenic liposomes (ELIPs), prepared following a particular protocol, has been demonstrated by others and us,[36,52−60] the exact mechanism of the echogenicity remains unknown. For ELIPs, repeated freeze−thaw cycles followed by lyophilization in the presence of mannitol in the preparation protocol has proved crucial for ensuring echogenicity.[36,61] It has been speculated that mannitol, being a weak cryoprotectant, leaves defects in the bilayer that during rehydration generate lipid-coated air-bubbles either inside liposomes or in the bilayer.[62,63] The bubbles, stabilized against dissolution by the coating,[64−66] produce strong ultrasound echoes. The lack of echogenicity in degassed solution as well as the strong nonlinear response verifies the role of bubbles in the acoustic response of echogenic polymersomes.

Figure 11A shows the enhancements at different excitation frequencies. The enhancement in fundamental response is strongest at 5 MHz excitation, whereas the highest subharmonic enhancement appears at 2.25 MHz. The latter

DOI: 10.1021/acs.biomac.8b01133
Biomacromolecules 2018, 19, 4122−4132

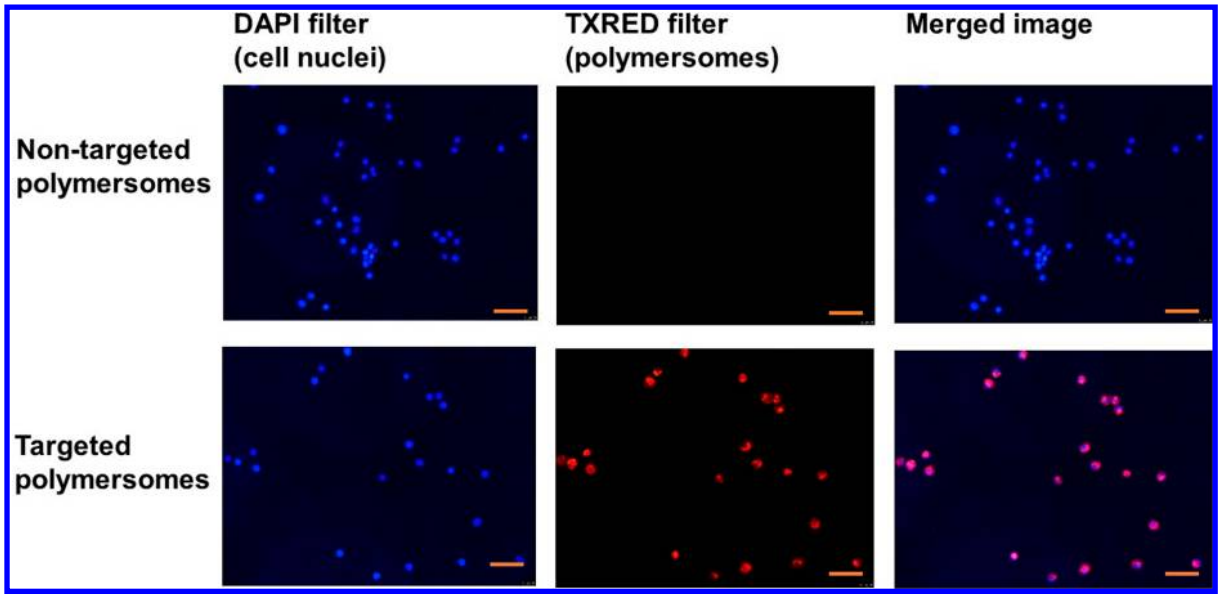

Figure 13. Cellular uptake studies with the BxPC3 cells. The nontargeted polymersomes (top panel) did not enter the cell nucleus. The targeted polymersomes (bottom panel) were present in the cell nuclei after 3 h of incubation (indicated by the overlapping blue and red colors in the Merged panel; scale bar: 50 μm).

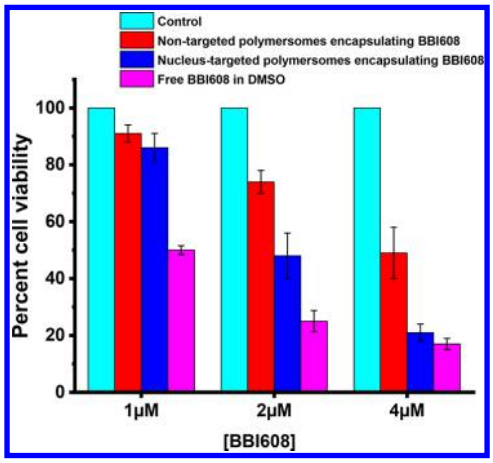

Figure 14. Viability of the BxPC3 cells in monolayer cultures at three different concentrations of encapsulated BBI608. Cell viability with media only (control, cyan bar), nontargeted polymersomes (red bar), nucleus-targeted polymersomes encapsulating BBI608 (blue bar), and free BBI608 (magenta bar, $N = 4$).

indicates the possibility of polymersome aided subharmonic imaging.[36,67] We also examined the scattered responses over a 20 min period in Figure 11B to investigate the long-term stability of their echogenicity crucial for clinical applications. During the 20 min sonication, the polymersomes produced an almost constant signal indicating their suitability for use in contrast-enhanced imaging. Polymersomes in degassed solution expectedly did not generate any scattered response.

Glutathione cleaves the disulfide bond destabilizing the bilayer of the polymersomes. We repeated the scattering experiments in the presence of 50 mM GSH. As expected, we observed that the fundamental enhancement decreased by 10 dB, and the subharmonic enhancement decreased by 4 dB (Figure 12) due to the loss of structural integrity of the polymersomes.

Nuclear Uptake Studies. To determine the localization within the pancreatic cancer cells, we prepared the polymersomes incorporating 5% of the DSPE−lissamine rhodamine lipid (structure shown in Figure 2) into the bilayer. We anticipated that the dexamethasone would dilate the nuclear pore complexes and transport the polymersomes inside the nucleus.[68] We incubated the BxPC3 pancreatic cancer cells with nucleus-targeted and nontargeted polymersomes for 3 h. Subsequently, the cell nuclei were stained with the HOESCHT 33342 dye and imaged employing a fluorescence microscope (Figure 13). We observed localization of the targeted polymersomes in the nuclei of the BxPC3 cells. We also observed similar results employing the breast cancer cells MCF-7 (Supporting Information).

Viability Studies in Monolayer Cultures of Pancreatic Cancer Cells. After validating efficient nuclear localization, we proceeded to determine the effectiveness of the nucleus-targeted, drug-encapsulated polymersomes in the pancreatic cancer cells. The monolayer culture of the BxPC3 cells was treated with the nucleus-targeted polymersomes encapsulating BBI608, the nontargeted vesicles, and the free drug for 48 h. The cell viability was determined by the Alamar Blue assay (Figure 14). We observed that the control polymersomes without the dexamethasone group decreased the cell viability to 50% at 4 μM concentration of encapsulated BBI608 (red columns). At this concentration of encapsulated drug, the targeted polymersomes were more effective, decreasing the viability of the BxPC3 cells to 21% (blue column), similar to the unencapsulated free BBI608 (pink columns). At lower concentrations of encapsulated BBI608 (1 and 2 μM), both encapsulated and free BBI608 were less effective in killing the cancer cells. We determined the IC_{50} values of the nucleus-targeted polymersomes encapsulating BBI608, the nontargeted vesicles, and the free drug for the BxPC3 cells (48 h) to be 1.75 ± 0.12, 3.20 ± 0.47, and 0.77 ± 0.48 μM, respectively (Supporting Information).

Viability Studies in Three-Dimensional Spheroid Cultures of Pancreatic Cancer Cells. Compared to the monolayer cultures, the spheroids demonstrate cellular heterogeneity, cell−cell interactions, and better mimic real

DOI: 10.1021/acs.biomac.8b01133
Biomacromolecules 2018, 19, 4122−4132

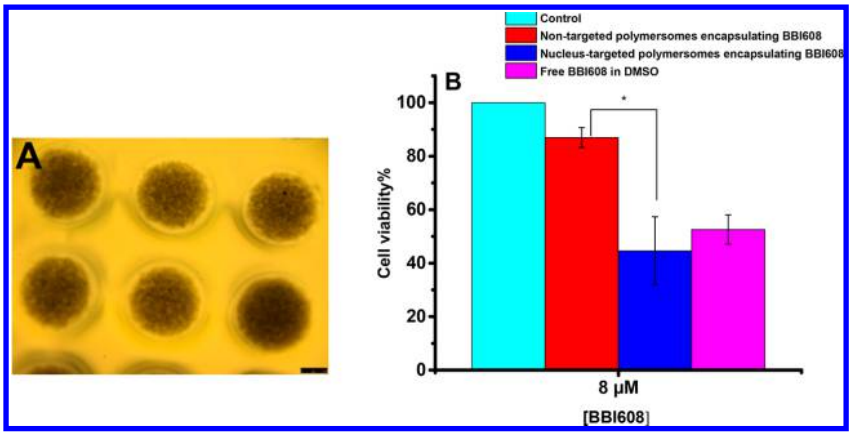

Figure 15. (A) Optical microscopic image of the 7-day old three-dimensional spheroids of the BxPC3 cells (scale bar: 25 μm). (B) Viability of the BxPC3 cells in spheroid cultures. Viability with media only (control, cyan bar), nontargeted polymersomes (red bar), nucleus-targeted polymersomes encapsulating BBI608 (blue bar), and the free BBI608 (magenta bar, $N = 4$).

tumors.[45,69] To evaluate the effectiveness of the polymersome formulations, BxPC3 spheroids were prepared using the 24-well 3D Petri dishes (Microtissues). We treated the 7-day old spheroids of the BxPC3 cells (Figure 15A) with nucleus-targeted polymersomes encapsulating BBI608, nontargeted polymersomes encapsulating BBI608, and free drug for 48 h. The cell viability was determined by the Alamar Blue assay. We observed that the nucleus-targeted polymersomes encapsulating BBI608 decreased ($p \leq 0.05$) the cell viability to 43% in compared to nontargeted polymersomes (84%) and the control (Figure 15B). We speculate that dexamethasone in the composition of polymersomes opens the nucleus pores, the vesicles enter the nuclei and release the cancer stemness inhibitor, leading to the enhanced toxicity in the BxPC3 cells.

CONCLUSIONS

We successfully synthesized alkyne dexamethasone and conjugated it to the N_3−PEG_{1900}−PLA_{8000} polymer. The nucleus-targeted polymer was combined with a redox-sensitive polymer to form stable polymeric vesicles, which encapsulate air bubbles and a stemness inhibitor. Our echogenic nucleus-targeted polymersomes respond to ultrasound and release the encapsulated BBI608 to the nucleus of pancreatic cancer cells. The nucleus-targeted drug-encapsulated polymersomes reduced the viability of pancreatic cancer cells in monolayer and spheroidal cultures to 30% and 43%, respectively. The polymersomes scatter ultrasound and respond to medical ultrasound imager, confirming the echogenicity. They have the potential to image and deliver chemotherapeutic drugs to the tumors tissues simultaneously. This is a noninvasive strategy to monitor targeted drug delivery to improve the therapeutic outcome of chemotherapy. The results of this research will pave the way for other ultrasound reflective nanoparticles for targeted drug delivery and simultaneous imaging capability.

ASSOCIATED CONTENT

Supporting Information

The Supporting Information is available free of charge on the ACS Publications website at DOI: 10.1021/acs.biomac.8b01133.

NMR spectra of the alkyne dexamethasone and the dexamethasone−PEG_{1900}−PLA_{8000} polymer, NMR spectra, and gel permeation chromatography of the N_3−PEG_{1900}−PLA_{8000} polymer (PDF).

AUTHOR INFORMATION

Corresponding Author

*E-mail: sanku.mallik@ndsu.edu. Phone: 701-231-7888. Fax: 701-231-7831.

ORCID

Sanku Mallik: 0000-0003-4236-2512

Funding

This research was supported by the NSF Grant DMR 1306154, and the NIH Grant 1 R01GM 114080 to S.M. and K.S. S.M. also acknowledges support from the Grand Challenge Initiative and the Office of the Vice President for Research and Creative Activity, North Dakota State University. We acknowledge Dr. Michael D. Scott for recording and interpreting the NMR spectrum of the alkyne−dexamethasone conjugate.

Notes

The authors declare no competing financial interest.

REFERENCES

(1) Karandish, F.; Mallik, S. Biomarkers and targeted therapy in pancreatic cancer. *Biomarkers Cancer* **2016**, *8* (Suppl 1), 27.

(2) Li, Y.; Rogoff, H. A.; Keates, S.; Gao, Y.; Murikipudi, S.; Mikule, K.; Leggett, D.; Li, W.; Pardee, A. B.; Li, C. J. Suppression of cancer relapse and metastasis by inhibiting cancer stemness. *Proc. Natl. Acad. Sci. U. S. A.* **2015**, *112* (6), 1839−1844.

(3) Zhang, Y.; Jin, Z.; Zhou, H.; Ou, X.; Xu, Y.; Li, H.; Liu, C.; Li, B. Suppression of prostate cancer progression by cancer cell stemness inhibitor napabucasin. *Cancer Med.* **2016**, *5* (6), 1251−1258.

(4) Hubbard, J. M.; Grothey, A. Napabucasin: An Update on the First-in-Class Cancer Stemness Inhibitor. *Drugs* **2017**, *77* (10), 1091−1103.

(5) Ganta, S.; Devalapally, H.; Shahiwala, A.; Amiji, M. A review of stimuli-responsive nanocarriers for drug and gene delivery. *J. Controlled Release* **2008**, *126* (3), 187−204.

(6) Mohammadi, M.; Ramezani, M.; Abnous, K.; Alibolandi, M. Biocompatible polymersomes-based cancer theranostics: Towards multifunctional nanomedicine. *Int. J. Pharm.* **2017**, *519* (1−2), 287−303.

(7) Leong, J.; Teo, J. Y.; Aakalu, V. K.; Yang, Y. Y.; Kong, H. Engineering Polymersomes for Diagnostics and Therapy. *Adv. Healthcare Mater.* **2018**, *7* (8), e1701276.

(8) Guan, L.; Rizzello, L.; Battaglia, G. Polymersomes and their applications in cancer delivery and therapy. *Nanomedicine (London, U. K.)* **2015**, *10* (17), 2757−80.

DOI: 10.1021/acs.biomac.8b01133
Biomacromolecules 2018, 19, 4122−4132

(9) Martin, C.; Aibani, N.; Callan, J. F.; Callan, B. Recent advances in amphiphilic polymers for simultaneous delivery of hydrophobic and hydrophilic drugs. *Ther. Delivery* **2016**, *7* (1), 15−31.
(10) Qin, Y.; Zhang, Z.; Huang, C.; Fan, F.; Liu, L.; Lu, L.; Wang, H.; Liu, Z.; Yang, J.; Wang, C.; Yang, H.; Sun, H.; Leng, X.; Kong, D.; Zhang, L.; Zhu, D. Folate-Targeted Redox-Responsive Polymersomes Loaded with Chemotherapeutic Drugs and Tariquidar to Overcome Drug Resistance. *J. Biomed. Nanotechnol.* **2018**, *14* (10), 1705−1718.
(11) Swain, S.; Sahu, P. K.; Beg, S.; Babu, S. M. Nanoparticles for Cancer Targeting: Current and Future Directions. *Curr. Drug Delivery* **2016**, *13* (8), 1290−1302.
(12) Thambi, T.; Park, J. H.; Lee, D. S. Stimuli-responsive polymersomes for cancer therapy. *Biomater. Sci.* **2016**, *4* (1), 55−69.
(13) Chen, W.; Meng, F.; Cheng, R.; Zhong, Z. pH-Sensitive degradable polymersomes for triggered release of anticancer drugs: a comparative study with micelles. *J. Controlled Release* **2010**, *142* (1), 40−46.
(14) Amstad, E.; Kim, S. H.; Weitz, D. A. Photo-and thermoresponsive polymersomes for triggered release. *Angew. Chem.* **2012**, *124* (50), 12667−12671.
(15) Kulkarni, P.; Haldar, M. K.; You, S.; Choi, Y.; Mallik, S. Hypoxia-Responsive Polymersomes for Drug Delivery to Hypoxic Pancreatic Cancer Cells. *Biomacromolecules* **2016**, *17* (8), 2507−2513.
(16) Kamat, N. P.; Robbins, G. P.; Rawson, J.; Therien, M. J.; Dmochowski, I. J.; Hammer, D. A. A generalized system for photoresponsive membrane rupture in polymersomes. *Adv. Funct. Mater.* **2010**, *20* (16), 2588−2596.
(17) Zhu, D.; Fan, F.; Huang, C.; Zhang, Z.; Qin, Y.; Lu, L.; Wang, H.; Jin, X.; Zhao, H.; Yang, H.; Zhang, C.; Yang, J.; Liu, Z.; Sun, H.; Leng, X.; Kong, D.; Zhang, L. Bubble-generating polymersomes loaded with both indocyanine green and doxorubicin for effective chemotherapy combined with photothermal therapy. *Acta Biomater.* **2018**, *75*, 386.
(18) Sarkar, B.; Paira, P. Theranostic Aspects: Treatment of Cancer by Nanotechnology. *Mini-Rev. Med. Chem.* **2018**, *18* (11), 969−975.
(19) Xu, P.; Van Kirk, E. A.; Zhan, Y.; Murdoch, W. J.; Radosz, M.; Shen, Y. Targeted Charge-Reversal Nanoparticles for Nuclear Drug Delivery. *Angew. Chem., Int. Ed.* **2007**, *46* (26), 4999−5002.
(20) Shahin, V.; Albermann, L.; Schillers, H.; Kastrup, L.; Schafer, C.; Ludwig, Y.; Stock, C.; Oberleithner, H. Steroids dilate nuclear pores imaged with atomic force microscopy. *J. Cell. Physiol.* **2005**, *202* (2), 591−601.
(21) Kastrup, L.; Oberleithner, H.; Ludwig, Y.; Schafer, C.; Shahin, V. Nuclear envelope barrier leak induced by dexamethasone. *J. Cell. Physiol.* **2006**, *206* (2), 428−34.
(22) Conrad, M.; Moreno, S.; Sinowatz, F.; Ursini, F.; Kölle, S.; Roveri, A.; Brielmeier, M.; Wurst, W.; Maiorino, M.; Bornkamm, G. The nuclear form of phospholipid hydroperoxide glutathione peroxidase is a protein thiol peroxidase contributing to sperm chromatin stability. *Mol. Cell. Biol.* **2005**, *25* (17), 7637−7644.
(23) Go, Y.-M.; Jones, D. P. Redox Control Systems in the Nucleus: Mechanisms and Functions. *Antioxid. Redox Signaling* **2010**, *13* (4), 489−509.
(24) Anajafi, T.; Scott, M. D.; You, S.; Yang, X.; Choi, Y.; Qian, S. Y.; Mallik, S. Acridine orange conjugated polymersomes for simultaneous nuclear delivery of gemcitabine and doxorubicin to pancreatic cancer cells. *Bioconjugate Chem.* **2016**, *27* (3), 762−771.
(25) Molineux, G. Pegylation: engineering improved pharmaceuticals for enhanced therapy. *Cancer Treat. Rev.* **2002**, *28*, 13−16.
(26) Chen, W. L.; Liu, S. J.; Leng, C. H.; Chen, H. W.; Chong, P.; Huang, M. H. Disintegration and cancer immunotherapy efficacy of a squalane-in-water delivery system emulsified by bioresorbable poly-(ethylene glycol)-block-polylactide. *Biomaterials* **2014**, *35* (5), 1686−95.
(27) Shah, S. S.; Zhu, K. J.; Pitt, C. G. Poly-DL-lactic acid: polyethylene glycol block copolymers. The influence of polyethylene glycol on the degradation of poly-DL-lactic acid. *J. Biomater. Sci., Polym. Ed.* **1994**, *5* (5), 421−31.
(28) Yang, W.; Zou, Y.; Meng, F.; Zhang, J.; Cheng, R.; Deng, C.; Zhong, Z. Efficient and Targeted Suppression of Human Lung Tumor Xenografts in Mice with Methotrexate Sodium Encapsulated in All-Function-in-One Chimeric Polymersomes. *Adv. Mater.* **2016**, *28* (37), 8234−8239.
(29) Wu, J.; Deng, C.; Meng, F.; Zhang, J.; Sun, H.; Zhong, Z. Hyaluronic acid coated PLGA nanoparticulate docetaxel effectively targets and suppresses orthotopic human lung cancer. *J. Controlled Release* **2017**, *259* (Supplement C), 76−82.
(30) Fang, Y.; Jiang, Y.; Zou, Y.; Meng, F.; Zhang, J.; Deng, C.; Sun, H.; Zhong, Z. Targeted glioma chemotherapy by cyclic RGD peptide-functionalized reversibly core-crosslinked multifunctional poly-(ethylene glycol)-*b*-poly(ε-caprolactone) micelles. *Acta Biomater.* **2017**, *50* (Supplement C), 396−406.
(31) Zhu, Y.; Wang, X.; Zhang, J.; Meng, F.; Deng, C.; Cheng, R.; Feijen, J.; Zhong, Z. Exogenous vitamin C boosts the antitumor efficacy of paclitaxel containing reduction-sensitive shell-sheddable micelles in vivo. *J. Controlled Release* **2017**, *250* (SupplementC), 9−19.
(32) Cheng, R.; Feng, F.; Meng, F.; Deng, C.; Feijen, J.; Zhong, Z. Glutathione-responsive nano-vehicles as a promising platform for targeted intracellular drug and gene delivery. *J. Controlled Release* **2011**, *152* (1), 2−12.
(33) García-Giménez, J. L.; Markovic, J.; Dasí, F.; Queval, G.; Schnaubelt, D.; Foyer, C. H.; Pallardó, F. V. Nuclear glutathione. *Biochim. Biophys. Acta, Gen. Subj.* **2013**, *1830* (5), 3304−3316.
(34) Huang, S.-L. Liposomes in ultrasonic drug and gene delivery. *Adv. Drug Delivery Rev.* **2008**, *60* (10), 1167−1176.
(35) Nahire, R.; Haldar, M. K.; Paul, S.; Mergoum, A.; Ambre, A. H.; Katti, K. S.; Gange, K. N.; Srivastava, D.; Sarkar, K.; Mallik, S. Polymer-coated echogenic lipid nanoparticles with dual release triggers. *Biomacromolecules* **2013**, *14* (3), 841−853.
(36) Paul, S.; Russakow, D.; Nahire, R.; Nandy, T.; Ambre, A. H.; Katti, K.; Mallik, S.; Sarkar, K. In vitro measurement of attenuation and nonlinear scattering from echogenic liposomes. *Ultrasonics* **2012**, *52* (7), 962−969.
(37) Huang, S.-L. Ultrasound-responsive liposomes. *Methods Mol. Biol.* **2010**, *605*, 113−128.
(38) Nahire, R.; Hossain, R.; Patel, R.; Paul, S.; Meghnani, V.; Ambre, A. H.; Gange, K. N.; Katti, K. S.; Leclerc, E.; Srivastava, D. pH-triggered echogenicity and contents release from liposomes. *Mol. Pharmaceutics* **2014**, *11* (11), 4059−4068.
(39) Paul, S.; Nahire, R.; Mallik, S.; Sarkar, K. Encapsulated microbubbles and echogenic liposomes for contrast ultrasound imaging and targeted drug delivery. *Computational Mech.* **2014**, *53* (3), 413−435.
(40) Nahire, R.; Haldar, M. K.; Paul, S.; Ambre, A. H.; Meghnani, V.; Layek, B.; Katti, K. S.; Gange, K. N.; Singh, J.; Sarkar, K. Multifunctional polymersomes for cytosolic delivery of gemcitabine and doxorubicin to cancer cells. *Biomaterials* **2014**, *35* (24), 6482−6497.
(41) Zhang, S.; Zhao, Y. Controlled release from cleavable polymerized liposomes upon redox and pH stimulation. *Bioconjugate Chem.* **2011**, *22* (4), 523−528.
(42) Discher, B. M.; Won, Y. Y.; Ege, D. S.; Lee, J. C.; Bates, F. S.; Discher, D. E.; Hammer, D. A. Polymersomes: tough vesicles made from diblock copolymers. *Science* **1999**, *284* (5417), 1143−6.
(43) Nahire, R.; Haldar, M. K.; Paul, S.; Ambre, A. H.; Meghnani, V.; Layek, B.; Katti, K. S.; Gange, K. N.; Singh, J.; Sarkar, K.; Mallik, S. Multifunctional polymersomes for cytosolic delivery of gemcitabine and doxorubicin to cancer cells. *Biomaterials* **2014**, *35* (24), 6482−97.
(44) Kopechek, J. A.; Abruzzo, T. M.; Wang, B.; Chrzanowski, S. M.; Smith, D. A.; Kee, P. H.; Huang, S.; Collier, J. H.; McPherson, D. D.; Holland, C. K. Ultrasound-Mediated Release of Hydrophilic and Lipophilic Agents From Echogenic Liposomes. *J. Ultrasound Med.* **2008**, *27* (11), 1597−1606.
(45) Karandish, F.; Haldar, M. K.; You, S.; Brooks, A. E.; Brooks, B. D.; Guo, B.; Choi, Y.; Mallik, S. Prostate-Specific Membrane Antigen

DOI: 10.1021/acs.biomac.8b01133
Biomacromolecules 2018, 19, 4122−4132

Targeted Polymersomes for Delivering Mocetinostat and Docetaxel to Prostate Cancer Cell Spheroids. *ACS omega* **2016**, *1* (5), 952−962.
(46) Mi Bae, Y.; Choi, H.; Lee, S.; Ho Kang, S.; Tae Kim, Y.; Nam, K.; Sang Park, J.; Lee, M.; Sig Choi, J. Dexamethasone-conjugated low molecular weight polyethylenimine as a nucleus-targeting lipopolymer gene carrier. *Bioconjugate Chem.* **2007**, *18* (6), 2029−36.
(47) Schnelldorfer, T.; Gansauge, S.; Gansauge, F.; Schlosser, S.; Beger, H. G.; Nussler, A. K. Glutathione depletion causes cell growth inhibition and enhanced apoptosis in pancreatic cancer cells. *Cancer* **2000**, *89* (7), 1440−1447.
(48) Schafer, F. Q.; Buettner, G. R. Redox environment of the cell as viewed through the redox state of the glutathione disulfide/glutathione couple. *Free Radical Biol. Med.* **2001**, *30* (11), 1191−1212.
(49) Redmond, S. M.; Joncourt, F.; Buser, K.; Ziemiecki, A.; Altermatt, H.-J.; Fey, M.; Margison, G.; Cerny, T. Assessment of P-glycoprotein, glutathione-based detoxifying enzymes and O6-alkylguanine-DNA alkyltransferase as potential indicators of constitutive drug resistance in human colorectal tumors. *Cancer Res.* **1991**, *51* (8), 2092−2097.
(50) Forsberg, F.; Shi, W. T.; Goldberg, B. Subharmonic imaging of contrast agents. *Ultrasonics* **2000**, *38* (1), 93−98.
(51) Sarkar, K.; Shi, W. T.; Chatterjee, D.; Forsberg, F. Characterization of ultrasound contrast microbubbles using in vitro experiments and viscous and viscoelastic interface models for encapsulation. *J. Acoust. Soc. Am.* **2005**, *118* (1), 539−550.
(52) Huang, S. L.; Hamilton, A. J.; Nagaraj, A.; Tiukinhoy, S. D.; Klegerman, M. E.; Mcpherson, D. D.; Macdonald, R. C. Improving ultrasound reflectivity and stability of echogenic liposomal dispersions for use as targeted ultrasound contrast agents. *J. Pharm. Sci.* **2001**, *90* (12), 1917−1926.
(53) Huang, S. L. Liposomes in ultrasonic drug and gene delivery. *Adv. Drug Delivery Rev.* **2008**, *60* (10), 1167−1176.
(54) Kopechek, J. A.; Haworth, K. J.; Raymond, J. L.; Mast, T. D.; Perrin, S. R.; Klegerman, M. E.; Huang, S. L.; Porter, T. M.; McPherson, D. D.; Holland, C. K. Acoustic characterization of echogenic liposomes: Frequency-dependent attenuation and backscatter. *J. Acoust. Soc. Am.* **2011**, *130* (5), 3472−3481.
(55) Coussios, C. C.; Holland, C. K.; Jakubowska, L.; Huang, S. L.; MacDonald, R. C.; Nagaraj, A.; McPherson, D. D. In vitro characterization of liposomes and Optison (R) by acoustic scattering at 3.5 MHz. *Ultrasound Med. Biol.* **2004**, *30* (2), 181−190.
(56) Kee, P.; Abruzzo, T.; Smith, D. A. B.; Wang, B.; Huang, S. L.; MacDonald, R. C.; Holland, C. K.; McPherson, D. D. Synthesis and acoustic characterization of a novel ultrasound controlled drug delivery system based on echogenic liposomes. *J. Am. Coll. Cardiolog.* **2007**, *49* (9), 120a−120a.
(57) Paul, S.; Nahire, R.; Mallik, S.; Sarkar, K. Encapsulated microbubbles and echogenic liposomes for contrast ultrasound imaging and targeted drug delivery. *Computational Mechanics* **2014**, *53* (3), 413−435.
(58) Nahire, R.; Paul, S.; Scott, M. D.; Singh, R. K.; Muhonen, W. W.; Shabb, J.; Gange, K. N.; Srivastava, D. K.; Sarkar, K.; Mallik, S. Ultrasound Enhanced Matrix Metalloproteinase-9 Triggered Release of Contents from Echogenic Liposomes. *Mol. Pharmaceutics* **2012**, *9* (9), 2554−2564.
(59) Nahire, R.; Hossain, R.; Patel, R.; Paul, S.; Meghnani, V.; Ambre, A. H.; Gange, K. N.; Katti, K. S.; Leclerc, E.; Srivastava, D. K.; Sarkar, K.; Mallik, S. pH-Triggered Echogenicity and Contents Release from Liposomes. *Mol. Pharmaceutics* **2014**, *11* (11), 4059−4068.
(60) Nahire, R.; Haldar, M. K.; Paul, S.; Mergoum, A.; Ambre, A. H.; Katti, K. S.; Gange, K. N.; Srivastava, D. K.; Sarkar, K.; Mallik, S. Polymer-Coated Echogenic Lipid Nanoparticles with Dual Release Triggers. *Biomacromolecules* **2013**, *14* (3), 841−853.
(61) Huang, S.-L.; Hamilton, A. J.; Pozharski, E.; Nagaraj, A.; Klegerman, M. E.; McPherson, D. D.; MacDonald, R. C. Physical correlates of the ultrasonic reflectivity of lipid dispersions suitable as diagnostic contrast agents. *Ultrasound Med. Biol.* **2002**, *28* (3), 339−348.
(62) Huang, S. L.; McPherson, D. B.; MacDonald, R. C. A method to co-encapsulate gas and drugs in liposomes for ultrasound-controlled drug delivery. *Ultrasound Med. Biol.* **2008**, *34* (8), 1272−1280.
(63) Kopechek, J. A.; Haworth, K. J.; Raymond, J. L.; Douglas Mast, T.; Perrin, S. R.; Klegerman, M. E.; Huang, S.; Porter, T. M.; McPherson, D. D.; Holland, C. K. Acoustic characterization of echogenic liposomes: Frequency-dependent attenuation and backscatter. *J. Acoust. Soc. Am.* **2011**, *130* (5), 3472.
(64) Sarkar, K.; Katiyar, A.; Jain, P. Growth and dissolution of an encapsulated contrast microbubble. *Ultrasound Med. Biol.* **2009**, *35* (8), 1385−1396.
(65) Katiyar, A.; Sarkar, K.; Jain, P. Effects of Encapsulation Elasticity on the stability of an Encapsulated Microbubble. *J. Colloid Interface Sci.* **2009**, *336*, 519−525.
(66) Katiyar, A.; Sarkar, K. Stability analysis of an encapsulated microbubble against gas diffusion. *J. Colloid Interface Sci.* **2010**, *343* (1), 42−47.
(67) Shi, W. T.; Forsberg, F. Ultrasonic characterization of the nonlinear properties of contrast microbubbles. *Ultrasound Med. Biol.* **2000**, *26* (1), 93−104.
(68) Kastrup, L.; Oberleithner, H.; Ludwig, Y.; Schafer, C.; Shahin, V. Nuclear envelope barrier leak induced by dexamethasone. *J. Cell. Physiol.* **2006**, *206* (2), 428−434.
(69) Desoize, B.; Gimonet, D.; Jardiller, J. Cell culture as spheroids: an approach to multicellular resistance. *Anticancer Res.* **1997**, *18* (6A), 4147−4158.

DOI: 10.1021/acs.biomac.8b01133
Biomacromolecules 2018, 19, 4122−4132